AN EXPERIMENT IN CYCLOGENESIS PREDICTION BY A TWO-LEVEL MODEL

HANS ØKLAND

Meteorological Institute, Oslo, Norway

ABSTRACT

Although it is proved theoretically that a two-parameter model is capable of converting potential energy into kinetic, there has been some doubt about its ability to predict successfully the strong cyclogenesis often associated with this energy conversion. The experiment described in this paper is intended to be a contribution to the solution of this problem.

A two-level primitive equation model with constant static stability has been integrated for two cases characterized by typical baroclinic developments, and the results are compared to the barotropic forecasts for the same cases.

The two-level prognoses are not better than the barotropic in many respects, but they show that at least some baroclinic developments can be predicted by this model.

1. INTRODUCTION

The barotropic model is now fairly well tested. It has proved to be a useful tool in daily weather prediction, and shows a comparatively high average score, measured for instance by the mean correlation coefficient of the computed and observed height changes. It is somewhat surprising that this rather crude model of the atmosphere should turn out to be so successful, and on the other hand that more complicated models very often give insignificant improvements over the barotropic. This is especially the case with two-parameter models, which represent the first step toward a better description of the vertical structure of the atmosphere, and also are the simplest models capable of converting potential energy into kinetic energy.

At this point it may be worthwhile to discuss what improvements over the barotropic forecast should be considered to be significant. This question is, of course, connected with the use one intends to make of the forecast. A numerical prediction model may very well produce prognoses which are useful for one purpose, but quite unsatisfactory for another. Similarly, a mean correlation coefficient may not be a sufficient measure of the usefulness of a model, especially when we consider the baroclinic developments, by which we mean a pronounced non-barotropic change, caused chiefly by a conversion of potential energy into kinetic. These developments as a rule take place in a limited area and during a time interval varying from 12 to 24 hr. Outside this area, and before and after the development has taken place, the atmosphere seems to be barotropic to a high degree. Some of these baroclinic cases are very important for general weather forecasting because they are connected with extreme weather conditions. But since they are comparatively rare, it could very well be that a baroclinic model, although it handles these developments reasonably well, still shows a mean statistical score inferior to the barotropic.

It therefore seems advisable to consider specifically the forecasts for some of these baroclinic cases, instead of relying entirely on statistical measures for the merits of a model. A few investigations along these lines have been made. An excellent example is the experiment made by Gates and Riegel [1] who integrated two types of two-level filtered models and compared the results to the barotropic forecast. They found that the two-level models generally failed to predict baroclinic developments, and they blame this on the fact that certain terms were left out in the vorticity equation and/or that two levels in the vertical are not sufficient to describe the mechanism of these developments.

The question of sufficient resolution in the vertical direction seems to be the most important one from a general point of view. If two parameters (or two levels) are not sufficient, there is little use in trying to utilize two-parameter models in short-time weather prediction. If on the other hand the failure of a two-parameter model has chiefly other sources, one should expect similar deficiencies also in models with more than two levels.

The experiment described in this paper is an attempt to throw some light upon this question. A primitive equation model has been coded and run on an IBM 7094 computer at the U.S. Weather Bureau, using operational analyses as input data. With two tropospheric information levels and constant static stability the model is comparable to the most common type of filtered two-parameter models. The use of the primitive equation instead of the vorticity equation makes it unnecessary to use a filtering approximation and comparatively simple to include all terms in the equation of motion. Numerical instability offers a special difficulty when primitive equa-

789-641 O - 65 - 2

tions are used, but in other respects one should expect less computational errors than by a general balanced model, since the computations are simpler.

Two cases were tried, both characterized by strong baroclinic developments over North America where the data coverage is especially good. In order to test the importance of the vertical advection term in the equation of motion, one of the cases was also run with this term left out.

2. THE DIFFERENTIAL EQUATIONS

The 300- and 700-mb. surfaces were used as reference levels. In accordance with established practice we denote quantities defined in these levels by the subscripts 1 and 3 respectively. Let α be any such quantity. We then define

$$\hat{\alpha} \equiv \tfrac{1}{2}(\alpha_1+\alpha_3)$$

$$\alpha' \equiv \alpha_1-\alpha_3.$$

In each level values of kinetic energy, absolute vertical vorticity, horizontal divergence, and convective acceleration are computed from

$$K=\frac{1}{2}\mathbf{v}^2$$

$$\eta=m^2\mathbf{k}\cdot\nabla\times\frac{\mathbf{v}}{m}+f$$

$$\delta=m^2\nabla\cdot\frac{\mathbf{v}}{m}$$

$$\mathbf{A}=\mathbf{k}\times\eta\,\frac{\mathbf{v}}{m}+\nabla K+c\,\frac{\mathbf{v}'}{m}\,\delta_1,$$

where m is the map-scale factor, $\mathbf{k}$ a vertical unit vector, ∇ is the horizontal grad operator in a pressure surface, f the Coriolis parameter, $\mathbf{v}$ the horizontal vector velocity with the components u and v. The numerical value of the constant c is computed in Appendix 1.

The following relation was used as horizontal boundary condition

$$\omega_{p=0}=\omega_{p=1000}=0.$$

From this and the continuity equation it follows that $\hat{\delta}=0$, so that $m^{-1}\hat{\mathbf{v}}$ may be defined by a stream function at any time.

The governing equations are the three prognostic equations

$$\frac{\partial z'}{\partial t}=-m\hat{\mathbf{v}}\cdot\nabla z'-s\delta_1 \tag{1}$$

$$\frac{\partial}{\partial t}\left(\frac{\mathbf{v}_1}{m}\right)=\mathbf{k}\times\nabla\frac{\partial\Psi}{\partial t}-\frac{1}{2}(\mathbf{A}'+g\nabla z') \tag{2}$$

$$\frac{\partial}{\partial t}\left(\frac{\mathbf{v}_3}{m}\right)=\mathbf{k}\times\nabla\frac{\partial\Psi}{\partial t}+\frac{1}{2}(\mathbf{A}'+g\nabla z') \tag{3}$$

and the diagnostic equation

$$\nabla^2\left(\frac{\partial\Psi}{\partial t}\right)+\mathbf{k}\cdot\nabla\times\hat{\mathbf{A}}=0. \tag{4}$$

The numerical value of the constant s in (1) is derived in Appendix 1.

The lateral boundary condition was

$$\mathbf{v}_1\cdot\mathbf{n}=\mathbf{v}_3\cdot\mathbf{n}=0, \tag{5}$$

where $\mathbf{n}$ is a horizontal unit vector, normal to the lateral boundary.

The system (1) through (4) does not carry $\hat{z}$ as an independent variable. However, this quantity may be derived from the velocity fields at any time by means of the vertically integrated divergence equation:

$$g\nabla^2\hat{z}+\nabla\cdot\hat{\mathbf{A}}=0. \tag{6}$$

The boundary condition for this equation

$$\mathbf{n}\cdot\nabla\hat{z}=-g^{-1}\mathbf{n}\cdot\hat{\mathbf{A}} \tag{7}$$

is readily derived from (5) and the equation of motion.

Necessary for the existence of a solution of (6) and (7) is that the line integral of (7) along the boundary equals the surface integral of $-g^{-1}\nabla\cdot\hat{\mathbf{A}}$ over the entire domain of integration. This condition is automatically fulfilled on account of Stokes' theorem.

For further details in the derivation of this type of model, the reader is referred to the papers by Eliassen [2] and Smagorinsky [3 and 4].

The finite difference equations are listed in Appendix 2.

3. THE COMPUTATIONS

The domain of integration was a rectangular area consisting of 53 x 57 grid points on a polar stereographic map. The mesh width was 381 km. Input data were the numerical analyses and stream functions computed operationally at National Meteorological Center, U.S. Weather Bureau. The octagonal area covered by the analyses was placed symmetrically in the rectangular domain of integration, and the boundary points of the rectangular domain were all given a constant value equal to the mean value on the boundary of the octagon. The ring-shaped area between these two boundaries was then filled in by a null Laplacian field. This method of extrapolation gives spurious vorticity to the grid points on the octagonal boundary. Further, since the operational stream functions also were treated in this way, one should perhaps suspect that the initial balance was destroyed. However, this did not seem to be the case, and the reason probably was that the operational analyses had very weak gradients near the boundary.

The time increment was 15 min. A simple uncentered forward time step was taken as the first one.

After about 20 time steps small-scaled noise waves began to develop near the jet stream, and during the next 10 to 20 steps they spread over a large area, and in this area the meteorologically significant features were no longer recognizable. This could be remedied to some extent by breaking off the computation after about 16 steps and starting from then on by a new uncentered step. In this way it was possible to carry on for 36 hr., but the fields were then rather "ragged".

Equation (6) was solved at the end of each forecast in order to get $\hat{z}$ as output field.

4. RESULTS

Figure 1 shows the initial $\hat{z}$ map for December 29, 1962, 1200 GMT, obtained from the objective analyses of the 300- and the 700-mb. surfaces.* Figure 2 shows the two-level 36-hr. prognosis, and figure 3 the verification map of $\hat{z}$, while figure 4 is the barotropic 500-mb. forecast, computed operationally at the National Meteorological Center, U.S. Weather Bureau. Two circumstances make this barotropic forecast somewhat unsuited for a comparison with the two-level model. First, the initial data for the barotropic forecast are the 500-mb. analysis, which is somewhat different from $\hat{z}$ (on the 500-mb. prognosis the lines are drawn for every 60 m., whereas the observed and predicted $\hat{z}$ fields are drawn for every 80 m.). Secondly, the barotropic model has mountain effect and long-wave control (Cressman [5], [6]), while these features are missing in the two-level model. However, we shall primarily be looking for the more pronounced differences, and particularly the baroclinic developments, and these features should be quite similar in the $\hat{z}$ field and the 500-mb. height field.

The prognostic z' fields, and also the 300- and 700-mb. forecasts were also contained in the output from the computer. These fields will not be shown, since they are considered to be of minor importance for the question dealt with in this paper.

A strong baroclinic development is seen to have taken place over North America, leading to a cut-off Low over New England. This development is well predicted by the two-level model, although it has deepened the Low a little too much.

A similar cyclogenesis has taken place over China, where a rather shallow trough has deepened into a strong Low. The two-level model has developed the Low, but it is much too weak. The two-level model has also created strong noise waves south and southeast of this area.

The Low in the western Pacific is moved into a more correct position by the two-level model than by the barotropic, but both models fail to predict the breakdown of the High farther to the north.

In the Greenland area there is a difference in favor of the barotropic forecast. This is probably caused by the mountain effect. More surprising are the errors which the two-level forecast has in the southeastern Atlantic. There are indications that these errors may be caused by an incorrect 300-mb. analysis, but this point will not be discussed here.

The initial map for the second case is shown in figure 5, while figures 6, 7, and 8 show the 36-hr. two-level forecast, the verification, and the 36-hr. barotropic forecast respectively. In this case, too, a baroclinic development has taken place over the United States, causing the high-level Low to be moved much farther to the southeast than predicted by the barotropic model. The two-level forecast shows a considerable improvement over the barotropic, although it has the cyclogenesis a little too far to the south. Also the Low south of Alaska has been brought in the correct position by the two-level model, while the barotropic forecast has it farther to the north. On the other hand the rather strong Low which the two-level model has developed over western Canada is almost missing on the verification map, and the barotropic forecast is much better in this area. This difference may also be caused by the mountain effect, but it is less obvious here than in the Greenland area in the other case.

Looking at other interesting features we may note that neither forecast has handled the trough east of Asia well, and that they also both fail to develop the ridge east of Iceland.

Figure 9 shows another 36-hr. prognosis for the December 29 case. The prognosis was made by means of the same two-level model, but the constant c in the equation of motion was set equal to zero. This change should have the same effect as omitting the twisting term and the vertical advection term in the vorticity equation. Comparing figure 9 and figure 2 it is obvious that there is no significant difference in the forecasts, and that especially the strong cyclogenesis over eastern United States is equally well predicted.

5. CONCLUSIONS

There are quite obviously serious errors in the two-level prognoses presented here. For one thing there is a lack of smoothness caused by the noise waves. Some sort of smoothing procedure would certainly improve the forecasts on this point. But apart from this there are also errors in the meteorologically significant part, and some of these errors are not present in the barotropic forecasts. To some extent this may be due to the mountain effect and possibly also the long-wave control in the barotropic model used for comparison. It should also be borne in mind that a barotropic model probably is less sensitive to analysis errors than a baroclinic, since its only energy source is the kinetic energy of a single tropospheric level.

However, the two-level forecasts are definitely better than the barotropic in some places, and especially over eastern North America where strong cyclogeneses have taken place. There is therefore little doubt that this

*The maps do not cover the whole domain of integration.

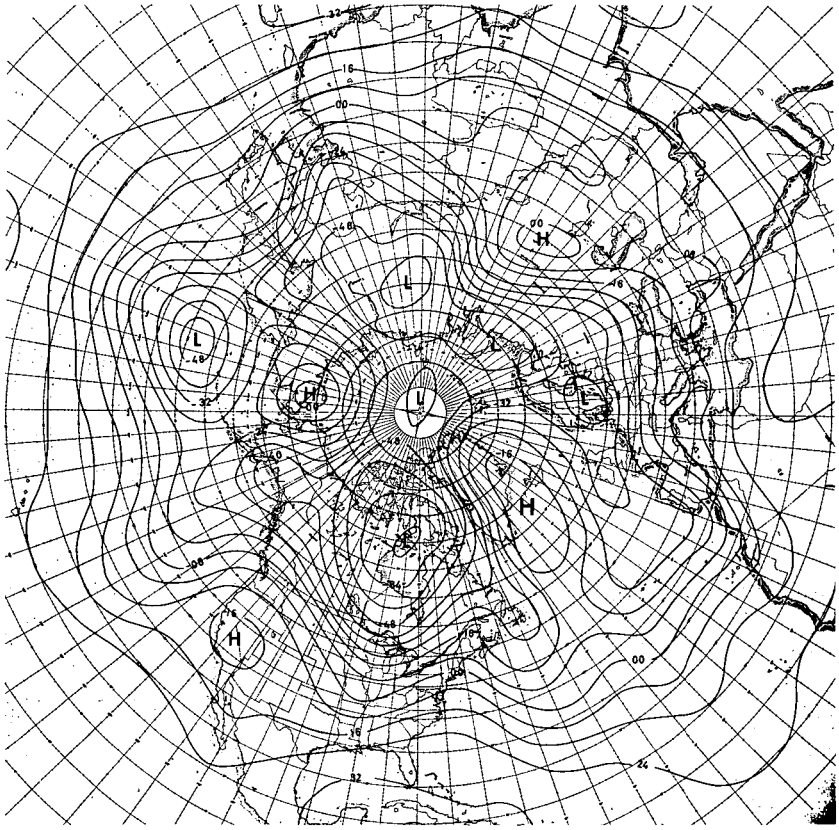

FIGURE 1.—Analysis of $\hat{z}$ for December 29, 1962, 1200 GMT.

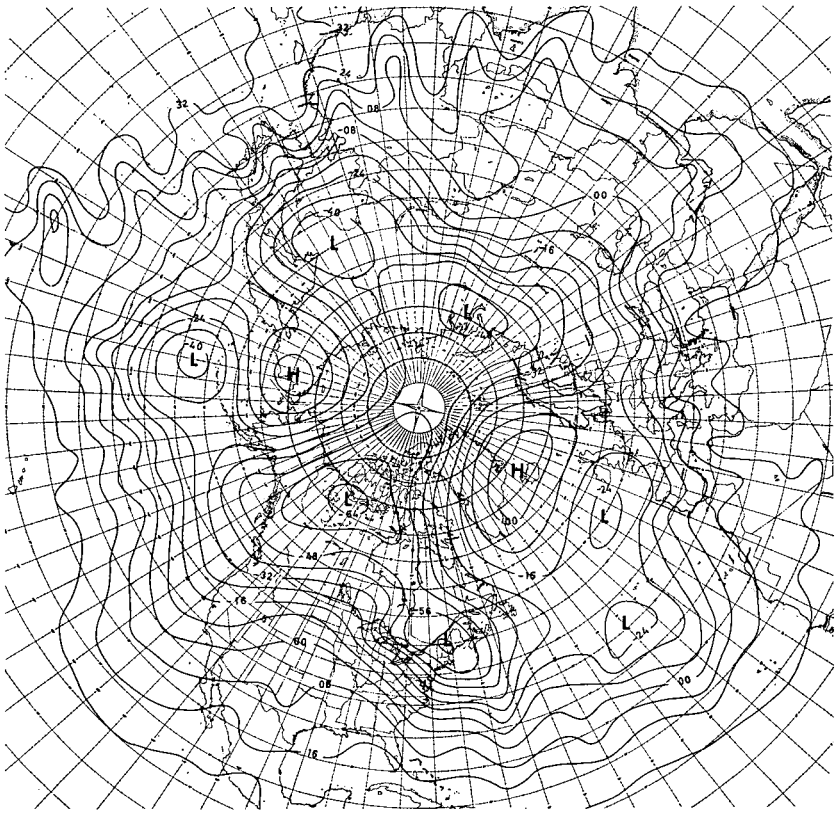

FIGURE 2.—Two-level 36-hr. prognosis of $\hat{z}$ from December 29, 1962, 1200 GMT.

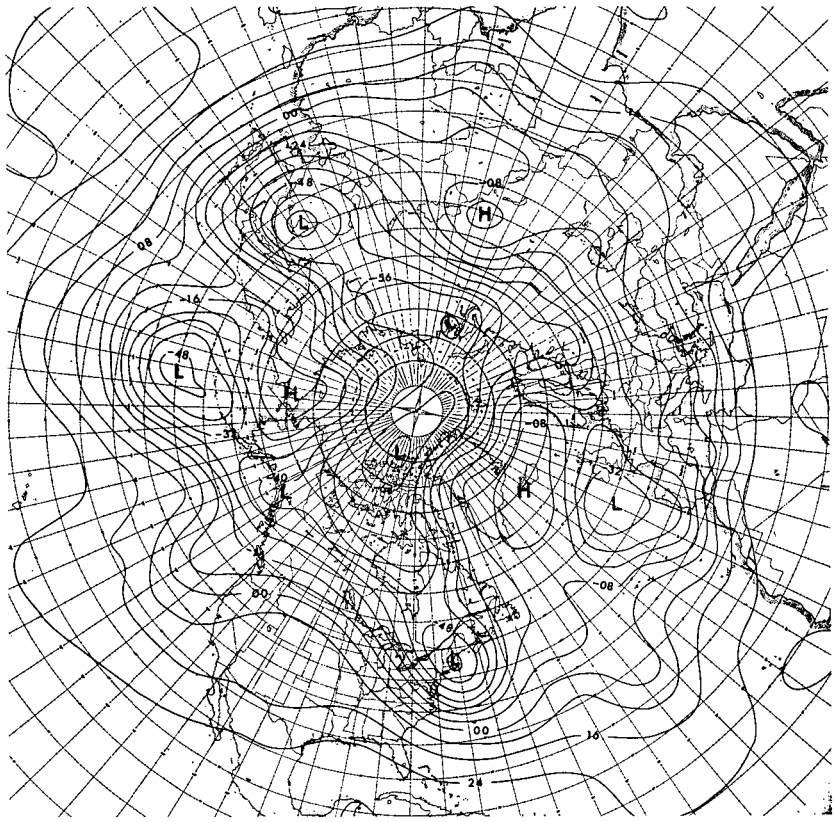

FIGURE 3.—Analysis of $\hat{z}$ for December 31, 1962, 0000 GMT.

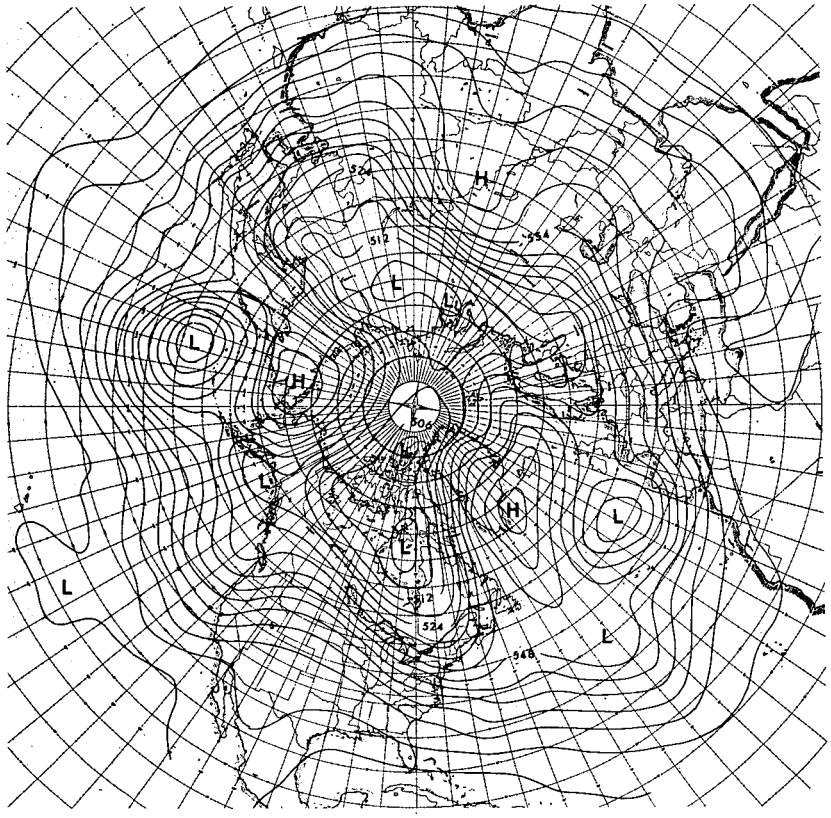

FIGURE 4.—Barotropic 36-hr. prognosis of 500-mb. contours from December 29, 1962, 1200 GMT.

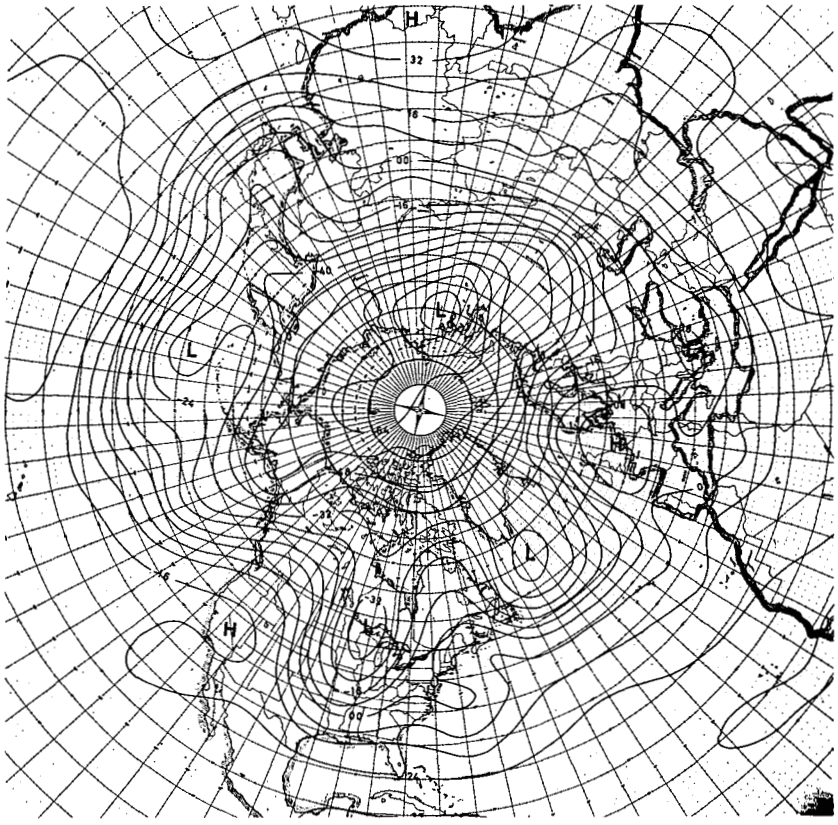

FIGURE 5.—Analysis of $\hat{z}$ for December 5, 1962, 1200 GMT.

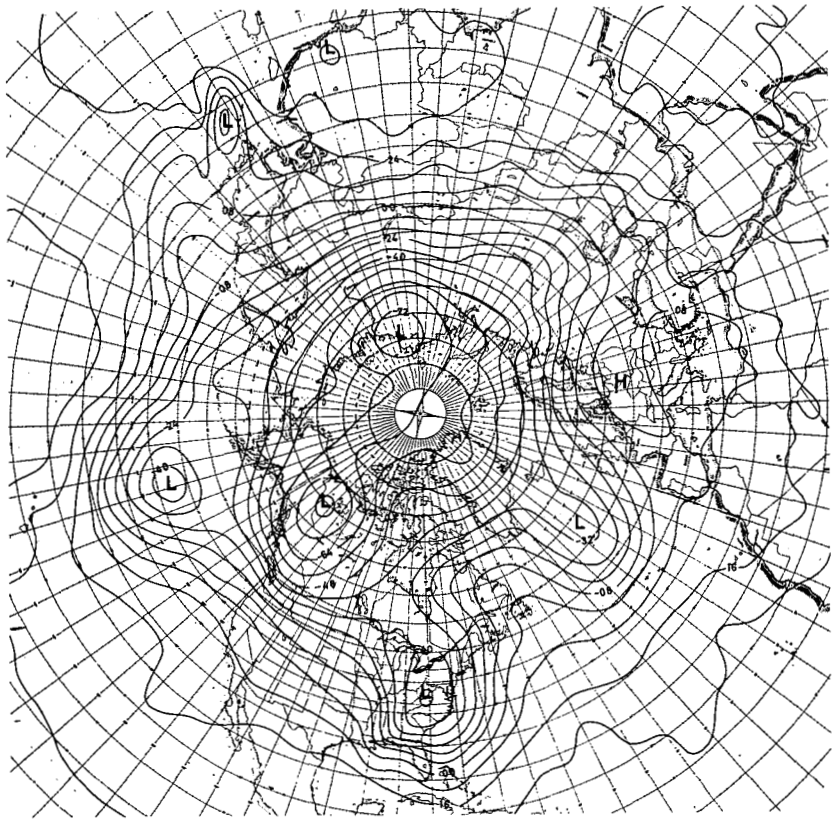

FIGURE 6.—Two-level 36-hr. prognosis of $\hat{z}$ from December 5, 1962, 1200 GMT.

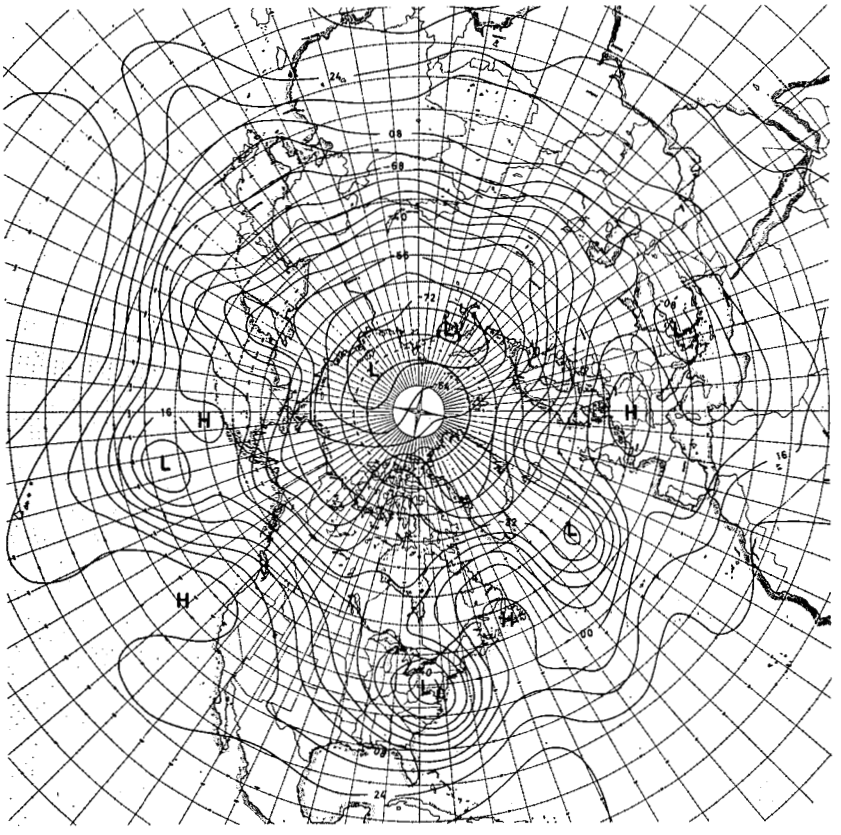

FIGURE 7.—Analysis of $\hat{z}$ for December 7, 1962, 0000 GMT.

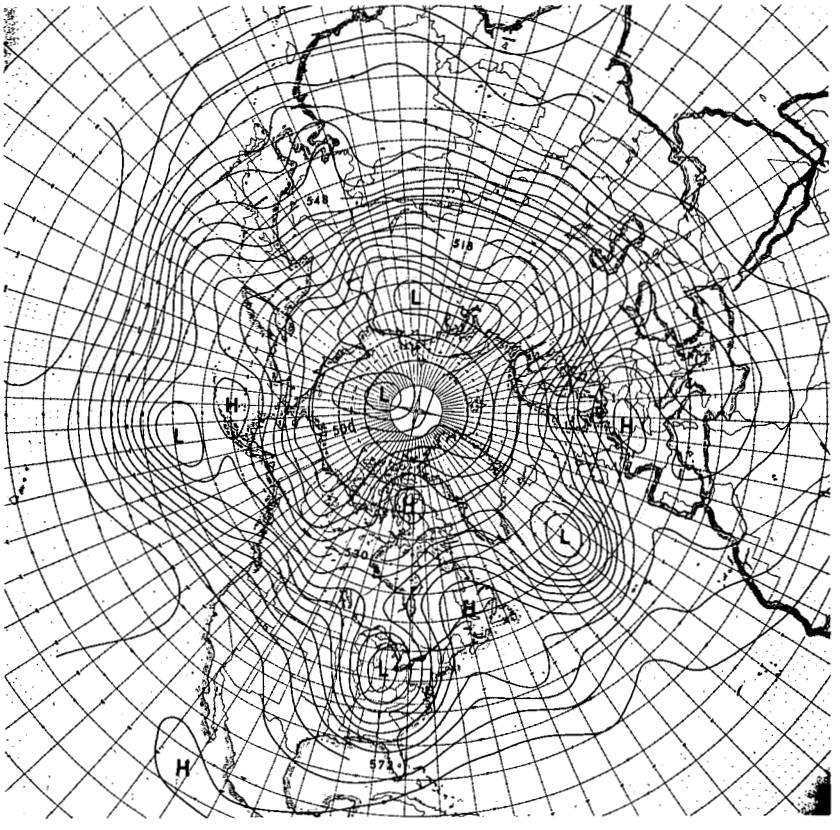

FIGURE 8.—Barotropic 36-hr. prognosis of 500-mb. contours from December 5, 1962, 1200 GMT.

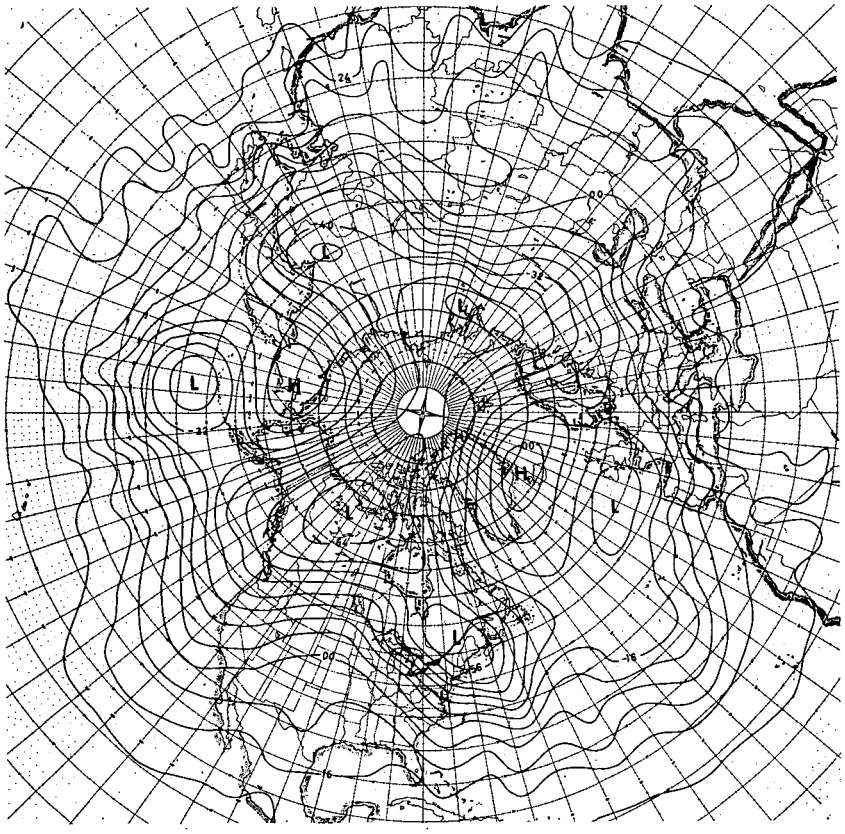

FIGURE 9.—Two-level 36-hr. prognosis of $\hat{z}$ from December 29, 1962, 1200 GMT. Vertical advection term neglected in the equation of motion.

two-level model is capable of predicting at least some of the significant baroclinic developments.

In one of the cases it was found that the vertical advection term in the equation of motion was of little importance for the forecast. In this form the model is little different from a simple geostrophic two-level model, and one could probably predict the cyclogenesis equally well with that type of model if the integration errors were kept sufficiently small.

ACKNOWLEDGMENT

This entire experiment was accomplished at National Meteorological Center, U.S. Weather Bureau. The author wishes to thank Dr. George P. Cressman and Dr. Frederick G. Shuman for their persistent interest and for profitable discussions.

APPENDIX 1.—NUMERICAL VALUES OF THE CONSTANTS

The constants c and s arise from the terms

$$\omega \frac{\partial \mathbf{v}}{\partial p} \tag{8}$$

and

$$-g^{-1} \int_{p_2}^{p_1} \omega \alpha \theta^{-1} \frac{\partial \theta}{\partial p} dp \tag{9}$$

in the dynamic and thermodynamic equation respectively. Finite difference approximations to these terms may be derived on the bases of special assumptions concerning the vertical variation of temperature and horizontal velocity. We shall here assume the variation of velocity to be linear with respect to pressure, and the variation of temperature to be linear with respect to height, i.e.,

$$\mathbf{v}=\hat{\mathbf{v}}+\frac{p-\hat{p}}{p'}\mathbf{v}' \tag{10}$$

$$\frac{\partial T}{\partial z}=\gamma \tag{11}$$

where γ is a constant.

From (10) one gets

$$\delta=2\frac{p-\hat{p}}{p'}\delta_1,$$

since $\hat{\delta}=0$ on account of the horizontal boundary condition. The continuity equation then gives

$$\omega=\delta_1\frac{2p\hat{p}-p^2}{p'}. \tag{12}$$

Inserting from (10) and (12) in (8) we finally get

$$\left(\omega\frac{\partial \mathbf{v}}{\partial p}\right)_1=\left(\omega\frac{\partial \mathbf{v}}{\partial p}\right)_3=c\delta_1\mathbf{v}'$$

with

$$c=\frac{\hat{p}^2-\left(\frac{p'}{2}\right)^2}{(p')^2},$$

which gives $c=1.3$ if $p_1=300$ mb. and $p_3=700$ mb.

Using (11), (12) and

$$\frac{1}{\theta}\frac{\partial\theta}{\partial p}=-\frac{R}{gp}\left(\frac{g}{c_p}+\gamma\right),$$

the term (9) may be expressed as $s\delta_1$ where

$$s=-\left(\frac{g}{c_p}+\gamma\right)\left(\frac{R}{g}\right)^2\hat{T}\left(1-2\frac{\hat{p}}{p'}\ln\left(\frac{p_1}{p_3}\right)\right).$$

With $\gamma=-0.006°$ m.$^{-1}$, $\hat{T}=252°$ K., $p_1=300$ mb. and $p_3=700$ mb., one gets $s=960$ m.

APPENDIX 2.—THE FINITE DIFFERENCE EQUATIONS

The basic principles used for constructing the finite difference approximations may be stated in this way: Compute the time increments of the dependent variables in the mid-point of the meshes, and then derive the value in the grid points by averaging over the four surrounding mid-points. A similar method has been used by Cressman [7] in connection with the Jacobian, and by Shuman [8] in his 4-level primitive equation model (personal communications). The procedure obviously has a smoothing effect on the tendencies of the shortest wave components described by the grid, and presumably suppresses the so-called non-linear instability. In the present model, however, the scheme did not turn out to be completely stable. This is described in section 3.

In the following we shall make use of mean and difference operators defined as

$$\overline{\alpha}^x\equiv\tfrac{1}{2}(\alpha_{i+\frac{1}{2},j,n}+\alpha_{i-\frac{1}{2},j,n})$$

$$\overline{\alpha}^y\equiv\tfrac{1}{2}(\alpha_{i,j+\frac{1}{2},n}+\alpha_{i,j-\frac{1}{2},n})$$

$$\alpha_x\equiv d^{-1}(\alpha_{i+\frac{1}{2},j,n}-\alpha_{i-\frac{1}{2},j,n})$$

$$\alpha_y\equiv d^{-1}(\alpha_{i,j+\frac{1}{2},n}-\alpha_{i,j-\frac{1}{2},n})$$

$$\overline{\alpha}^t_t\equiv(2\Delta t)^{-1}(\alpha_{i,j,n+1}-\alpha_{i,j,n-1})$$

The finite difference equations are listed below. Scaled velocity components, $U=um^{-1}$ and $V=vm^{-1}$, are used instead of the true values. Also note that the left-hand sides of the formulas (14) through (18) are defined in the mid-point of the meshes, whereas the other equations apply to the grid points.

$$K=\tfrac{1}{2}m^2(U^2+V^2) \tag{13}$$

$$\eta=(\overline{m}^{xy})^2(\overline{V}^y_x-\overline{U}^x_y)+\overline{f}^{xy} \tag{14}$$

$$\delta=(\overline{m}^{xy})^2(\overline{U}^y_x+V^x_y) \tag{15}$$

$$A=-\eta\overline{V}^{xy}+\overline{K}^y_x+c\overline{U'}^{xy}\delta_1 \tag{16}$$

$$B=\eta\overline{U}^{xy}+\overline{K}^x_y+c\overline{V'}^{xy}\delta_1 \tag{17}$$

$$H=(\overline{m}^{xy})^2\left(\overline{\hat{U}}^{xy}\overline{z}^y_x+\overline{\hat{V}}^{xy}\overline{z}^x_y\right) \tag{18}$$

$$\overline{z}'^t_t=\overline{-H-s\delta_1}^{xy} \tag{19}$$

$$\overline{(U_1)}^t_t=\overline{-\overline{(\Delta\Psi)}^x_y-\tfrac{1}{2}(A'+g\overline{z}'^y_x)}^{xy} \tag{20}$$

$$\overline{(V_1)}^t_t=\overline{\overline{(\Delta\Psi)}^y_x-\tfrac{1}{2}(B'+g\overline{z}'^x_y)}^{xy} \tag{21}$$

$$\overline{(U_3)}^t_t=\overline{-\overline{(\Delta\Psi)}^x_y+\tfrac{1}{2}(A'+g\overline{z}'^y_x)}^{xy} \tag{22}$$

$$\overline{(V_3)}^t_t=\overline{\overline{(\Delta\Psi)}^y_x+\tfrac{1}{2}(B'+g\overline{z}'^x_y)}^{xy} \tag{23}$$

$$\overline{(\Delta\Psi)}^{yy}_{xx}+\overline{(\Delta\Psi)}^{xx}_{yy}=-\overline{\hat{B}}^y_x+\overline{\hat{A}}^x_y \tag{24}$$

Equation (24) is derived from

$$\overline{\hat{U}}^t_t=-\overline{(\Delta\Psi)}^{xxy}_y=\overline{-\hat{A}-g\hat{z}_x}^{xy} \tag{25}$$

$$\overline{\hat{V}}^t_t=\overline{(\Delta\Psi)}^{xyy}_x=\overline{-\hat{B}-g\hat{z}_y}^{xy}. \tag{26}$$

The operator $\overline{(\,)}^x_y$ is applied to the first of these equations and the operator $\overline{(\,)}^y_x$ to the second. When the resulting equations are subtracted, the terms containing $\hat{z}$ drop out, and we finally get (24) by removing an operator $\overline{(\,)}^{xy}$.

It turns out that the operator $\overline{(\,)}^{yy}_{xx}+\overline{(\,)}^{xx}_{yy}$ reduces to

$$2^{-1}d^{-2}[(\,)_{i+1,j+1}+(\,)_{i-1,j+1}+(\,)_{i-1,j-1}+(\,)_{i+1,j-1}-4(\,)_{i,j}]. \tag{27}$$

The prognostic equations (19) through (23) cannot be computed for the grid points on the lateral boundary without special assumptions. For the left boundary ($i=0$) these assumptions are

$$(\Delta z')_{-\frac{1}{2},j}=(\Delta z')_{\frac{1}{2},j}$$

$$(\Delta U_1)_{-\frac{1}{2},j}=-(\Delta U_1)_{\frac{1}{2},j}$$

$$(\Delta V_1)_{-\frac{1}{2},j}=(\Delta V_1)_{\frac{1}{2},j}$$

$$(\Delta U_3)_{-\frac{1}{2},j}=-(\Delta U_3)_{\frac{1}{2},j}$$

$$(\Delta V_3)_{-\frac{1}{2},j}=(\Delta V_3)_{\frac{1}{2},j}$$

where $\Delta z'$, ΔU_1, ΔV_1, ΔU_3, ΔV_3 are the right-hand side of equations (19) through (23) without the space averaging $\overline{(\,)}^{xy}$. Similar relations are constructed for the other boundaries (the domain of integration is supposed to be rectangular). These assumptions are in agreement with the lateral boundary condition, from which we also deduce that $\Delta\Psi=0$ in all the boundary points.

A special property of the Poisson equation (24) should be noted. Because of the form of the operator (27), the system of algebraic equations which corresponds to (24) separates into two independent systems, each comprising every second grid point in both directions.

The finite difference form of (6)

$$g\left(\bar{\hat{z}}^{yy}_{xx}+\bar{\hat{z}}^{xx}_{yy}\right)=-\bar{\hat{A}}^{y}_{x}-\bar{\hat{B}}^{x}_{y} \tag{28}$$

is readily obtained from (25) and (26).

In order to derive the boundary condition (7) in difference form we first note that (28) may be rewritten as

$$(g\bar{z}^{yy}_{x})+\bar{A}^{y})_{x}+\overline{(g\bar{z}^{x}_{yy}+B_{y})}^{x}=0, \tag{29}$$

where the sign $\wedge$ has been omitted for the sake of simplicity. This equation is now applied to a point $(0, j)$ on the left boundary, assuming a fictitious row of points $(-1, j)$ outside the domain. On account of the boundary condition we get from (25)

$$\overline{g\bar{z}^{yy}_{x}+\bar{A}^{y}}^{x}=0 \tag{30}$$

and, since

$$(\Delta V)_{-\frac{1}{2},j}=(\Delta V)_{\frac{1}{2},j}$$

we also have

$$(g\bar{z}^{x}_{y}+B)_{x}=0. \tag{31}$$

Combining (29), (30), and (31) under consideration of the identity

$$\left(\frac{d}{2}\alpha_{x}+\bar{\alpha}^{x}\right)_{0,j}\equiv\alpha_{\frac{1}{2},j}$$

we get for a boundary point which is not at the same time a corner point

$$z_{1,j+1}+z_{1,j-1}-2z_{0,j}=-dg^{-1}(A_{\frac{1}{2},j+\frac{1}{2}}+A_{\frac{1}{2},j-\frac{1}{2}}+B_{\frac{1}{2},j+\frac{1}{2}}-B_{\frac{1}{2},j-\frac{1}{2}}).$$

For a corner point (e.g., the lower left) we get in a similar way

$$z_{1,1}-z_{0,0}=-dg^{-1}(A_{\frac{1}{2},\frac{1}{2}}+B_{\frac{1}{2},\frac{1}{2}}).$$

REFERENCES

1. W. Lawrence Gates and Christopher A. Riegel, "Comparative Numerical Integration of Simple Atmospheric Models on a Spherical Grid," *Tellus*, vol. 15, No. 4, Nov. 1963, pp. 406–423.
2. A. Eliassen, "A Procedure for Numerical Integration of the Primitive Equations of the Two-Parameter Model of the Atmosphere," *Scientific Report* No. 4 on contract AF19(604)–1286, University of California at Los Angeles, Dept. of Meteorology, Mar. 1956, 53 pp.
3. J. Smagorinsky, "On the Numerical Integration of the Primitive Equations of Motion for Baroclinic Flow in a Closed Region," *Monthly Weather Review*, vol. 86, No. 12, Dec. 1958, pp. 457–466.
4. J. Smagorinsky, "General Circulation Experiments with the Primitive Equations," *Monthly Weather Review*, vol. 91, No. 3, March 1963, pp. 99–164.
5. G. P. Cressman, "Barotropic Divergence and Very Long Atmospheric Waves," *Monthly Weather Review*, vol. 86, No. 8, Aug. 1958, pp. 293–297.
6. G. P. Cressman, "Improved Terrain Effects in Barotropic Forecasts," *Monthly Weather Review*, vol. 88, Nos. 9–12, Sept.–Dec. 1960, pp. 327–332.
7. G. P. Cressman, "A Three-Level Model Suitable for Daily Numerical Forecasting," *Technical Memorandum No. 22*, National Meteorological Center, U.S. Weather Bureau, 1963, pp. 10–11.
8. F. G. Shuman, "Numerical Experiments with the Primitive Equations," *Proceedings of the International Symposium on Numerical Weather Prediction in Tokyo, November 1960*, Meteorological Society of Japan, March 1962, pp. 85–106.

[*Received July 19, 1965; revised September 8, 1965*]